

*Research Paper*

## **Agricultural damage assessment for paddy fields from land use land cover and flood extent maps of five unions of Sunamganj using remote sensing-based analysis**

**S. S. Tasnim<sup>1\*</sup>, R. M. S. Hoque<sup>1</sup>, M. Y. Tarana<sup>1</sup> and M. M. Rahman<sup>1</sup>**

### **Abstract**

Flooding is a major issue in Bangladesh, and the severity of floods grows each year, resulting in fatalities, crop damage, and economic loss. A wave of high-intensity flash floods from the neighbouring country's mountains hit Bangladesh's Sylhet division in 2022. The research aimed to generate a map to identify the extent of floods during peak flood days in Sunamganj unions. Inundation images were gathered via the Google Earth Engine (GEE) platform, with threshold techniques used to detect flooded areas. During the primary data collection field visit, areas of four different categories—rivers, *haors*, paddy fields, and trees—were observed and pinpointed in Google Maps. They were then used to train classifiers in GEE to identify and classify each category to produce the land use/land cover (LULC) maps of pre- and post-flood events. Ground truthing was performed to determine the accuracy of the flood extension, duration, and agricultural loss. The flood extension map of the study area was found to be a close match to the map collected from the Flood Forecasting and Warning Centre (FFWC). A damage and economic loss assessment for affected vegetation areas was done using the flood extent map and the pre- and post-flood LULC maps. There was a significant change in LULC during flood events, particularly in paddy fields and *haors*. The study's findings estimate significant economic loss due to agricultural land damage. Maps of flooded areas of the kind produced in the study can help decision-makers take prompt action.

**Keywords:** Flood extent mapping, paddy field damage, land use/land cover, Google Earth Engine, spatial analysis.

### **1. Introduction**

Bangladesh is considered a land of rivers, consisting of 1,008 rivers (National River Conservation Commission, 2023). The three most common types of flooding in Bangladesh are flash floods, riverine floods, and coastal floods. Riverbank overflows due to the high volume of upstream water passing through rivers causing riverine floods in the monsoon season (Dadhich et al., 2019). When there is considerable rainfall in mountain areas, rainwater gushes through the mountains as a flash flood, creating abrupt and catastrophic inundation in the downstream areas. Because of poor drainage and a lack of green spaces, Bangladesh's increasing urbanization has increased the vulnerability of urban areas to flooding, endangering daily life, health, and safety of the community (Tanim & Mullick, 2017). Flash floods occur mostly in the north-eastern part of Bangladesh. During monsoon season, Sunamganj in the north-eastern Sylhet division becomes one of the districts most vulnerable to flash floods due to heavy rainfall (United

---

<sup>1</sup> North South University, Bashundhara, Dhaka-1129, Bangladesh.

\* Corresponding author. Email: [sheikh.tasnim01@northsouth.edu](mailto:sheikh.tasnim01@northsouth.edu)

News of Bangladesh, 2022; "Flood Situation", 2022; BSS, 2022). Normally, the rainy season of the monsoon starts in June and goes on until October. But, rainfall of the monsoon came early in March 2022, activating floods in Sunamganj during late April (Zahid, 2022). Flash floods occurred frequently after April, which resulted in flood inundation in mid-June. In 2022, parts of India's Assam and Meghalaya faced the highest amount of precipitation in decades. In total, 2,162 mm of rainfall occurred during the peak flood period of June 2022 (Mishra, 2023). People lost their agricultural crops, and homes and were highly exposed to waterborne diseases (Bangladesh Red Crescent Society, 2022).

The study of flood mapping is a cost and time-efficient approach especially in flood risk assessments (Gorsevski et al., 2006). This study utilized a few remote sensing approaches using software like ArcGIS Pro, Google Earth Engine (GEE), and ERDAS Imagine to analyse, classify, and modify satellite data. Sentinel 1A (SAR image) and Sentinel 2A (optical image) have been previously used in some research to study the flooding scenarios of Bangladesh using the GEE platform and other remote sensing tools but land use land cover classification and damage assessment using GEE for the selected flooding event or study area have not been done yet (Shermin, 2022; Pandey et al., 2022; Aziz et al., 2022). Sentinel 1A data is primarily used for mapping and surveillance tasks such as forest and agriculture management, disaster forecasting, and ocean and coastline inspection (Cossu et al., 2009). Sentinel 2A data have a high spatial and spectral resolution, frequent coverage, open data policy, multitemporal capabilities, and imagery quality making it well-suited for accurately detecting land surface characteristics and identifying changes related to land use, particularly those caused by floods (Dehni & Lounis, 2012). For data collection of flood extent and severity in Sunamganj from far away without being physically present in the area, the remote sensing approaches proved to be useful. Large areas can be captured repeatedly and quickly, and interpreting the images is less time-consuming and less expensive than conducting ground investigations (Ahmad & Munim, 2020). It is feasible to determine the exact land use/land cover (LULC) classes impacted among the inundated regions by overlapping the supervised land use map with the flood extent map (Haque & Basak, 2017). The magnitude of the land use land cover damage produced by a flood may be determined with great precision via supervised land use/land cover classification (Ge et al., 2020). GEE is an effective tool for mapping inundated zones, improving ongoing efforts to save lives, protect community-based livelihood, and preserve urban spaces and welfare (Mehmood et al. 2021). As a flexible cloud platform, GEE enables the implementation of pixel-based and object-oriented LULC classification strategies due to the availability of several cutting-edge features made up of different machine learning algorithms (Tassi & Vizzari, 2020).

The study aimed to assess the flood extent, LULC change, and impact on the paddy fields during the flooding event of June 2022 in Sunamganj district for the five selected unions of Sunamganj, which are Mannargaon, Pandergaon, Purba Pagla, Durgapasha and Kalkalia (Aziz et al., 2022). The flood extent map was validated statistically with the map of FFWC and a comparison between pre-flood LULC map and post-flood LULC map has been done. The research findings can be used as guidance for decision makers and

resource managers developing sustainable a flood management, mitigation of flood risks, damage, and community vulnerability (Rahman et al., 2021).

## 2. Methodology

### 2.1. Study area

The research was carried out in Sunamganj district of Sylhet division, which is situated in the northeastern part of Bangladesh (Figure 1). North side of the district is bounded by an Indian state named Meghalaya. Sunamganj has 16.28 km<sup>2</sup> of forests out of a total area of 3,747.2 km<sup>2</sup> and the total population is 2,695,495 (Hannan, 2021; Bangladesh Bureau of Statistics, 2022). The district consists of 11 upazilas (sub-districts) and 87 unions. For the purpose of this research, three upazilas were selected from which five unions were taken under observation. A list of selected unions is shown in Table 1.

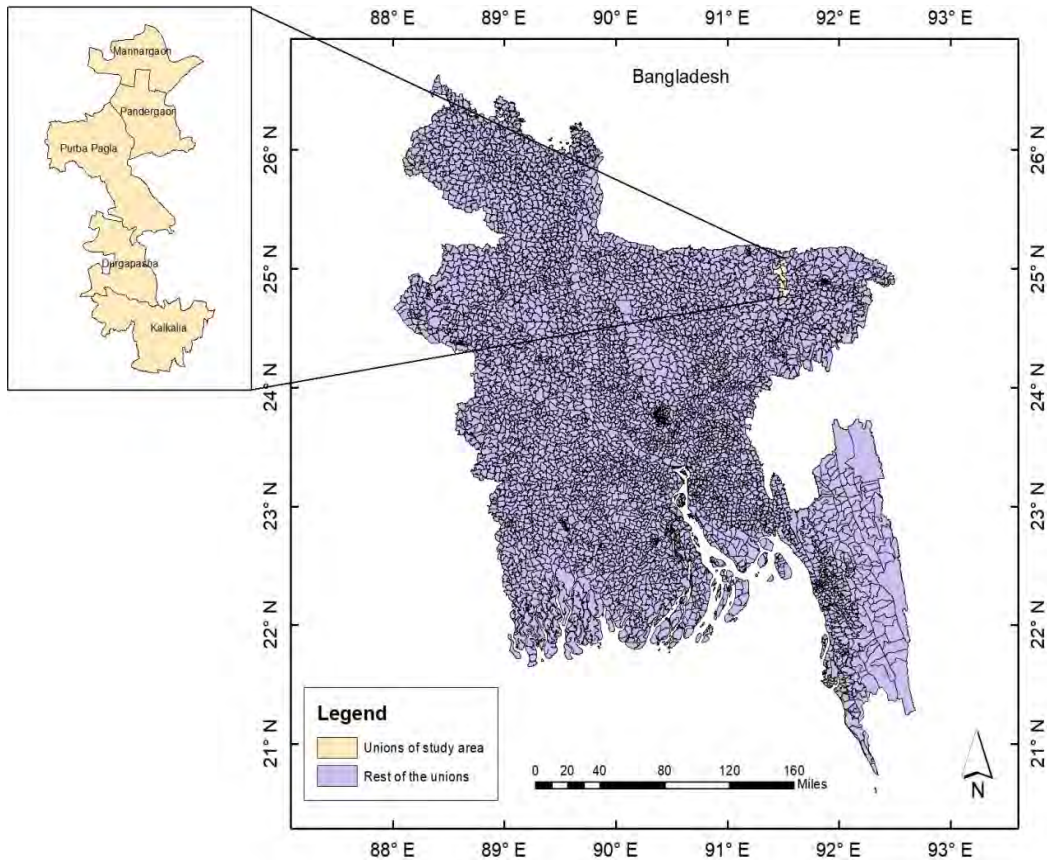


**Figure 1.** Map of the study area. Source: Authors (2023).

**Table 1.** Geographic locations of the study area.

| Division | District  | Upazila                           | Union       | Latitude     | Longitude    |
|----------|-----------|-----------------------------------|-------------|--------------|--------------|
| Sylhet   | Sunamganj | Dowara Bazaar                     | Mannargaon  | 25°03'59.8"N | 91°28'31.5"E |
| Sylhet   | Sunamganj | Dowara Bazaar                     | Pandergaon  | 24°58'32.3"N | 91°30'34.8"E |
| Sylhet   | Sunamganj | Dakshin Sunamganj<br>(Shantiganj) | Purba Pagla | 24°55'21.2"N | 91°29'37.6"E |
| Sylhet   | Sunamganj | Dakshin Sunamganj<br>(Shantiganj) | Durgapasha  | 24°53'03.8"N | 91°28'48.0"E |
| Sylhet   | Sunamganj | Jogannathpur                      | Kalkalia    | 24°49'59.8"N | 91°31'15.4"E |

## 2.2. Methodological flowchart

Figure 2 below outlines the overall methodology of the study.

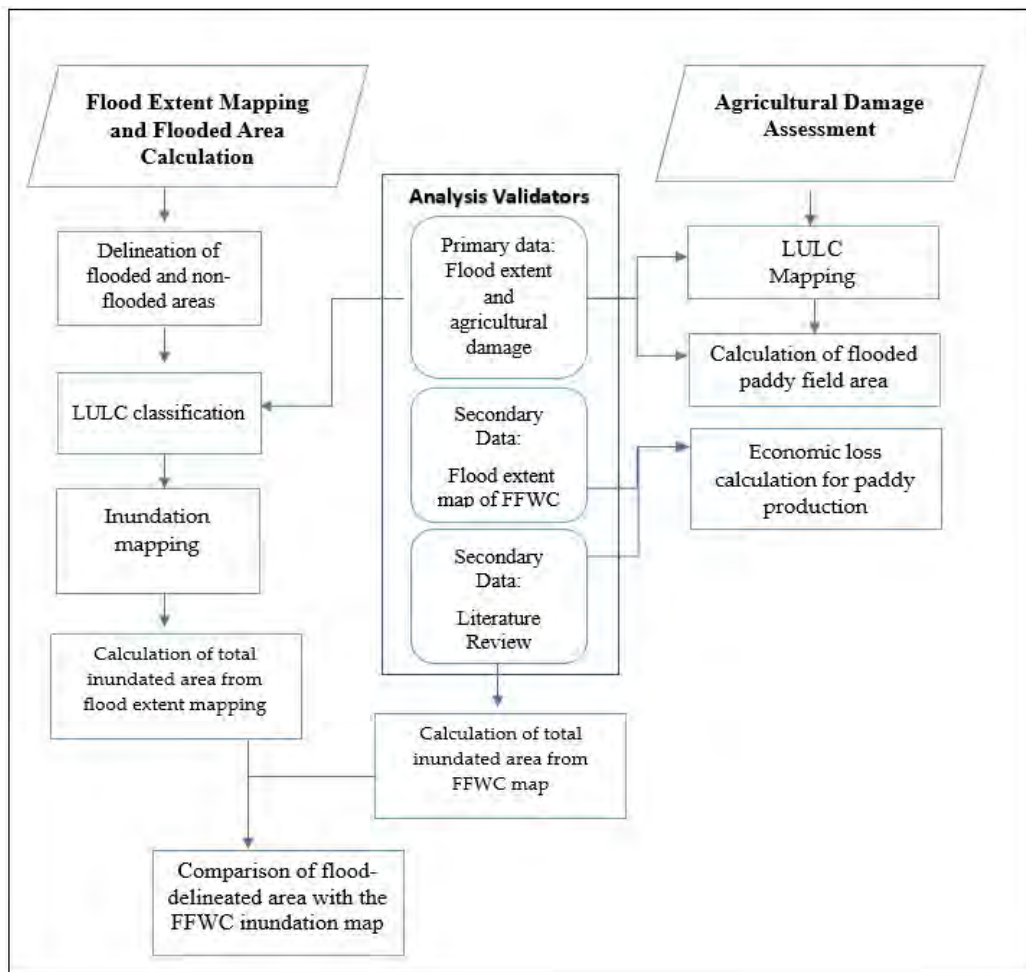


**Figure 2.** Methodological flowchart. Source: Authors (2023).

### 2.3. Primary data collection

The selection of upazilas for primary data collection was based on the severity of flood according to reports of multiple news portals (United News of Bangladesh, 2022; "Flood Situation," 2022; BSS, 2022). Key Informant Interview (KII) was conducted with the upazila executive officer (UNO, chief administrative officer of the upazila) of each selected union to gather information on the period of flood, estimated areas of vegetation lost due to flood, and the percentage of areas inundated. The river Surma which is periodically heavily flooded flows through the Doarabazar upazila, which makes it highly prone to flooding (BSS, 2022). The data collection process also involved physically going to different locations within the study area to verify and validate the land use and land cover classes assigned to different categories in the study. Using the satellite view of Google maps, twenty named landmarks (for example, schools and mosques) were selected from the five unions. The positions of selected land use types were pinpointed and later used to identify the corresponding pixel colours in GEE to produce a supervised LULC classified map.

### 2.4. Flood extent mapping

The flood extent mapping was done using GEE as it can tackle the obstacles of open analysis and cloud-free image downloading from a wide range of satellite products (Bégué et al., 2018). Statistical calculations can be also done to measure the area of extent based on multiple criteria (GIS Geography, 2023).

#### 2.4.1 Generation of flood map in Google Earth Engine

The following steps briefly describe the flood extent analysis (description of the Java codes are given in the appendix).

**Study area boundary extraction:** For the purpose of union specific analysis, every union shapefile was individually selected in the Google Earth Engine (GEE) JavaScript platform as area of interest from imported Bangladesh administrative boundary shape file obtained from the Humanitarian Data Exchange website.

**Image criteria selection and downloading:** GEE's Javascript code includes VH (Vertical/Horizontal) mode for transmitter-receiver polarization, as well as Interferometric Wide Swath (IW) mode for instrument polarization. The IW mode is specially made for acquiring imagery of terrain surfaces and offers stable archives for a lengthy period (Singha et al., 2020). The orbit property pass was set to both ascending and descending (mentioned in appendix).

Images were collected from the freely available Sentinel-1 SAR GRD: C-band Synthetic Aperture Radar database provided by the European Space Agency (ESA). SAR signals can penetrate clouds unlike in the case of Landsat; therefore, it is particularly useful in regions with cloud cover during the monsoon season. The time frame of the study was the first ten days of February and the last twenty days of June 2022. The pre- and post-flood periods were from 1 February to 10 February 2022 and from 10 June to 30 June 2022, respectively. The pre-flood period is in February because it is one of the driest seasons in the study area (Patrick, 2017) and the surface water signature is only limited to the permanent waterbodies. The period of 10 to 30 June 2022 for image selection was

because the flood started from 10 June, and water level kept increasing till 22 June 2022 (United News of Bangladesh, 2022; BSS, 2022; Debu, 2023).

**Image corrections:** The mosaic and clip functions were used to combine the data into one image and bound it. DB values were converted to natural, then the refined Lee function was used to remove noise and smoothen the image. It was then converted back to dB.

**Flood inundation identification:** The names 'flood\_mask' and 'water\_mask' were assigned to two classification functions. Flood\_mask is total flood inundated areas that can be seen to have a dB value less than -20 for pre-flood period and greater than -20 post-flood. Whereas water\_mask is the total surface water, river, etc. with a dB value less than -20 in both periods. Yellow and blue colours were assigned for specific layers of flood mask and water mask, representing 'flood\_inundation' and 'water' respectively.

**Flooded area calculation and exporting the map:** The total union area was calculated, from which the total flooded area was calculated and then converted from number of pixels to hectares. The maps were exported and then modified using ArcGIS Pro 10.6 because of its suitability for organizing, visualizing, and analysing spatial patterns of images in different layers for decision-making (GIS Cloud, 2022).

## 2.5. Land Use Land Cover (LULC) mapping

The LULC of the unions were classified and mapped using GEE. Harmonized Sentinel 2 satellite image collector was used for LULC classification. Unlike sentinel 1 SAR data, Sentinel 2 images have cloud cover limitations but are essential for detecting changes in spatial patterns of land use and land cover of any area (Singha et al., 2020). The period of acquisition of the images was from 10 February to 20 March 2022, like the dry season pre-flooded image shows. It was selected because this is the driest month of the year when there was no flooding in the study area. For identification of post-flooding LULC impact, images from 10 June 2022 to 30 June 2022 were selected. The following steps briefly describes the LULC analysis (description of the Java codes are given in the appendix).

### 2.5.1 Supervised classification using Google Earth Engine

The 'ROI' filters were used to select data from the study area. Variable 'L8' clipped a bound area, and filtered the date of the pre-flood period, for image collection. LULC is classified into four categories which are waterbody, haor, paddy field, and trees.

The coloured pixels for the paddy field in the GEE map were selected by point markers through satellite view. This selection was done based on the real-time pixel colour of the specific class, observed, and noted in Google Maps during the site visit. After adding true colour bands, the four classifiers were merged into a single feature collection. Training data were extracted from selected bands and then the classifiers were trained with the Smile Cart classifier.

The variable 'classified' defines the whole selected band of image collection, including classifiers. The code for the calculation of areas in classes was exported to and modified in ArcGIS Pro 10.6.

## 2.6. Flooded agricultural area calculation

The reclassified flood extent and LULC maps were exported to GIS and a map was

created showing the area of paddy fields that were flooded. The map of the flooded paddy field was converted from raster to polygon. The geographic coordinates were converted to the projected coordinate system to calculate the area. The total area of flooded paddy field in a union was calculated in hectares using the 'calculate geometry' function.

## 2.7. FFWC inundated area calculation

A map of inundated area from the Flood Forecasting and Warning Centre (FFWC) was used as secondary data to validate our inundation mapping. With the help of GIS, water bodies, flood inundated areas, and non-flooded areas were identified. The raster file was then converted to polygons and converted to a projected coordinate system. The rest of the steps of area calculation follows section 3.6.

## 3. Result and Discussion

### 3.1. Results

#### 3.1.1 Validation of map

The UNOs reported that the upazilas were almost totally inundated during peak flood. They confirmed that the twenty selected landmarks from five unions were inundated during the specific time for which the flood extent image was collected. It was found from the generated maps that 80% of the selected landmarks had been submerged and 20% were on unaffected land. Figures 3 displays the location of the four landmarks selected from each of the five unions spread across the three study upazilas.

The data obtained from the primary collection process for affected vegetated cultivable lands by the flood of 2022 is shown in Table 2. It can be seen that Purba Pagla, Kalkalia, and Durgapasha unions were the most affected in terms of cultivated land, while the damage was relatively milder in Manargaon and Pandergaon.

**Table 2.** Area of flood-affected land under vegetation cover by union.

| Union       | Affected area under vegetation (ha) |
|-------------|-------------------------------------|
| Mannargaon  | 50                                  |
| Pandergaon  | 20                                  |
| Purba Pagla | 3,500                               |
| Durgapasha  | 3,000                               |
| Kalkalia    | 3,200                               |

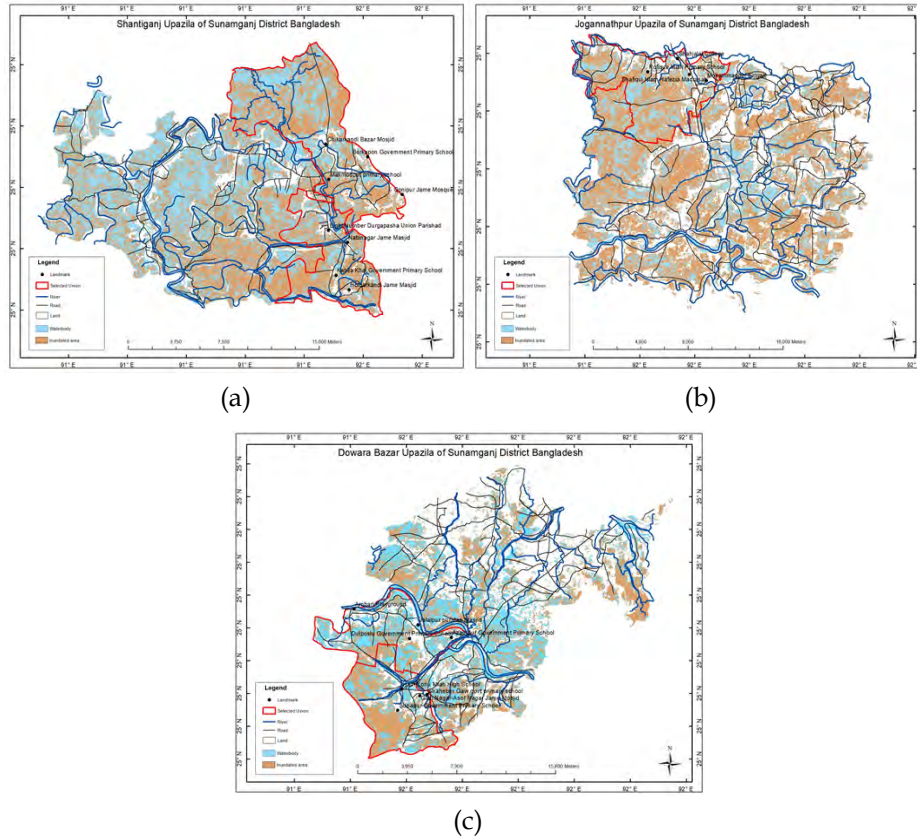


**Figure 3.** Area map of (a) Shantiganj upazila, (b) Jagannathpur upazila and (c) Dowara Bazar Upazila. Source: Authors (2023).

### 3.1.2 Inundation mapping

With the help of GEE and GIS, a satellite map has been created and classified for the unions of Sunamganj. The area of the union including flood extent and waterbody has been calculated. In this map, landmarks were included with three separate categories of land, which are waterbody, inundated areas, and non-flooded land.

The study area has a total area of 23,666 ha, of which 11,339 ha were inundated, represented in brown in Figure 4. The water bodies, shown in light blue, extend over 8,090 ha. Therefore, approximately 82% of the total study area was inundated (including permanent water bodies). Table 3 shows the total area, area of permanent water bodies and area inundated for the unions.



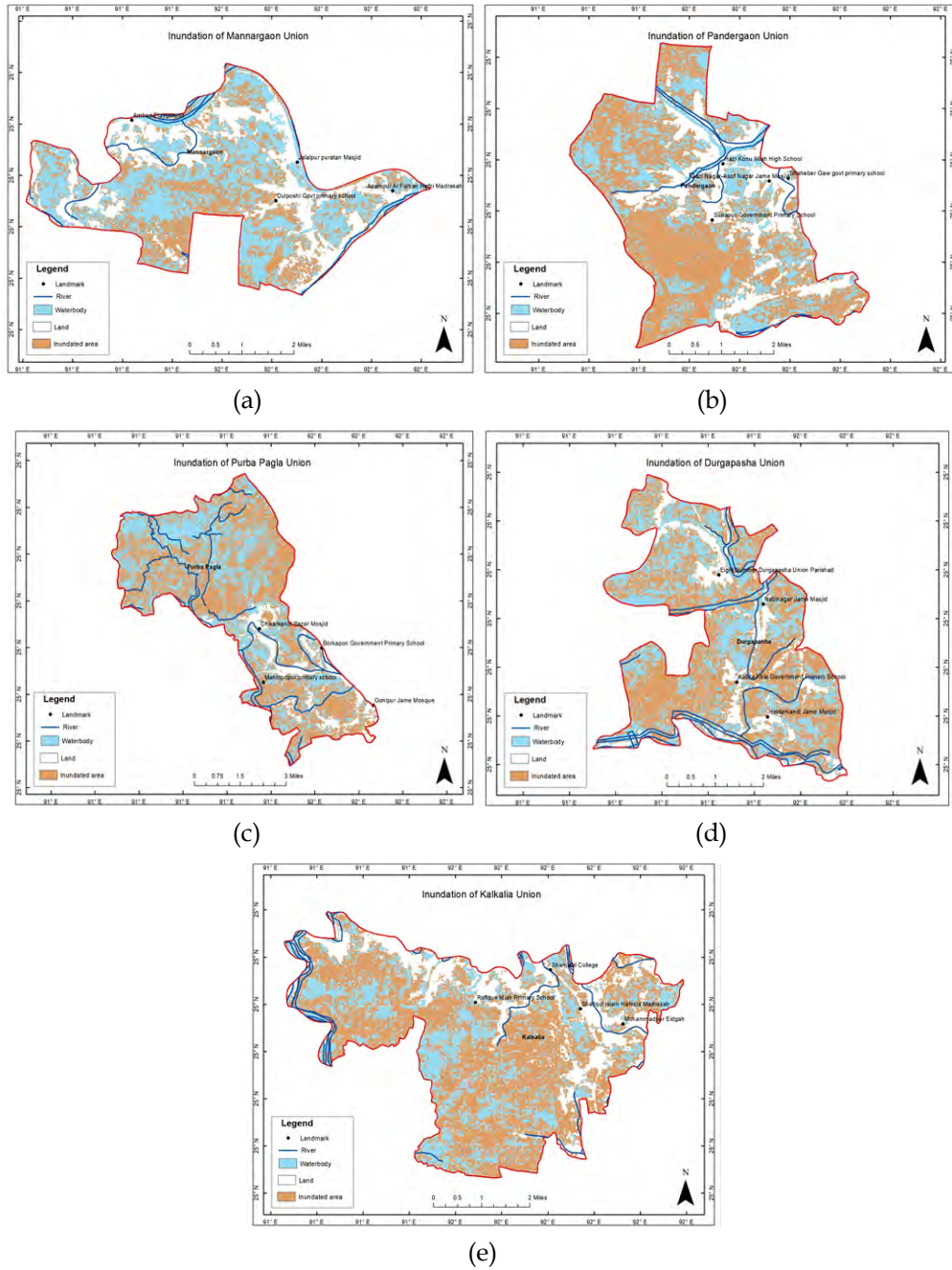


**Figure 4.** Flood extent maps of (a) Mannargaon Union, (b) Pandergaon Union, (c) Purba Pagla Union, (d) Durgapasha Union, and (e) Kalkalia Union. Source: Authors (2023).

**Table 3.** Total inundated area from flood extent mapping.

| Union       | Total union area (ha)<br><i>A</i> | Flooded area (ha)<br><i>F</i> | Permanent waterbody (ha)<br><i>P</i> | Total inundated area (ha)<br><i>I = F+P</i> | Percentage of total inundated area<br><i>I/A*100</i> |
|-------------|-----------------------------------|-------------------------------|--------------------------------------|---|--|
| Mannargaon  | 3,538                             | 1,048                         | 1,481                                | 2,529                                       | 71.5   |
| Pandergaon  | 3,809                             | 1,833                         | 1,115                                | 2,948                                       | 77.4   |
| Purba Pagla | 7,070                             | 3,566                         | 2,759                                | 6,325                                       | 89.5   |
| Durgapasha  | 3,854                             | 1,997                         | 1,298                                | 3,295                                       | 85.5   |
| Kalkalia    | 5,395                             | 2,895                         | 1,437                                | 4,332                                       | 80.0   |
| Total       | 23,666                            | 11,339                        | 8,090                                | 19,429                                      | 82.10  |

The total area of flood extent and waterbody according to the FFWC flood inundation map is given in Table 4 below.

**Table 4.** Total inundated area from FFWC map analysis.

| Union       | Total union area (ha) | Total inundated area (ha) | Percentage of total inundated area |
|-------------|-----------------------|---------------------------|------------------------------------|
| Mannargaon  | 3,538                 | 2,159                     | 61.02%                             |
| Pandergaon  | 3,809                 | 2,626                     | 68.94%                             |
| Purba Pagla | 7,070                 | 5,689                     | 80.46%                             |
| Durgapasha  | 3,854                 | 3,118                     | 80.9%                              |
| Kalkalia    | 5,395                 | 3,313                     | 61.41%                             |

A comparison of the inundation area as derived from the study analyses against that calculated from the FFWC map is given in the Figure 5 below. It shows that there is good correspondence between the two.

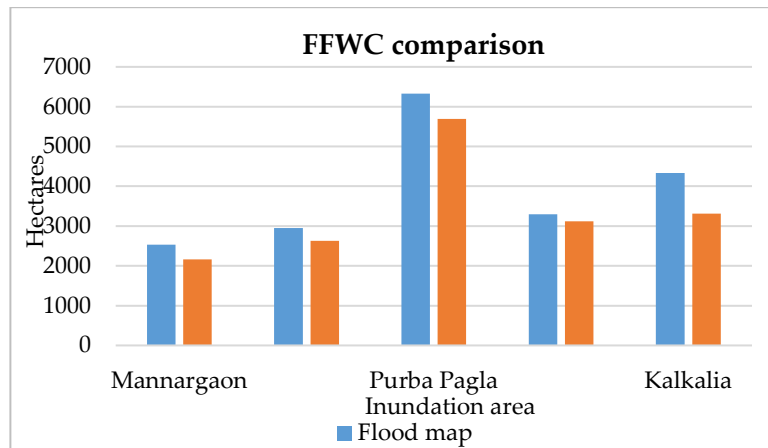


**Figure 5.** Comparison of total inundated areas of FFWC map and generated map. Source: Authors (2023).

### 3.1.3 LULC supervised classification

The LULC maps for pre- and post-flood periods were created. The LULC were classified into four categories: rivers, haors, paddy fields, and trees. Maps of the two periods from each union are given in Figures 6–10, and the areas under different classes are shown in Figure 11.

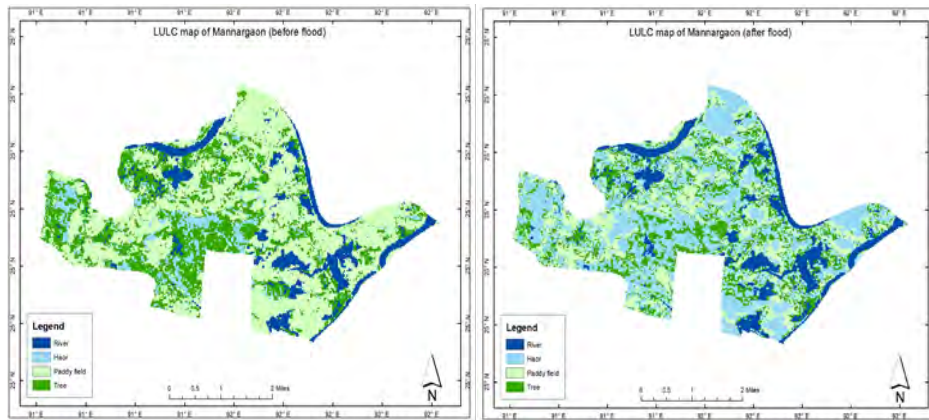


Figure 6. LULC map of Mannargaon before and after flood. Source: Authors (2023).

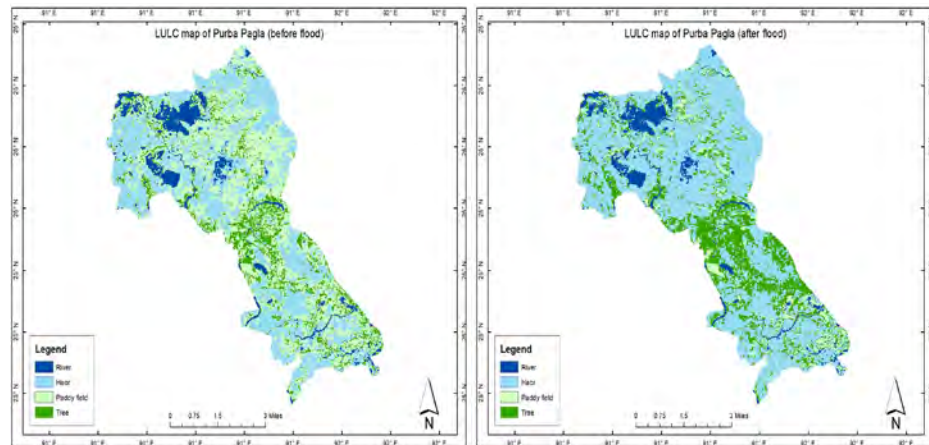


Figure 7. LULC map of Purba Pagla before and after flood. Source: Authors (2023).

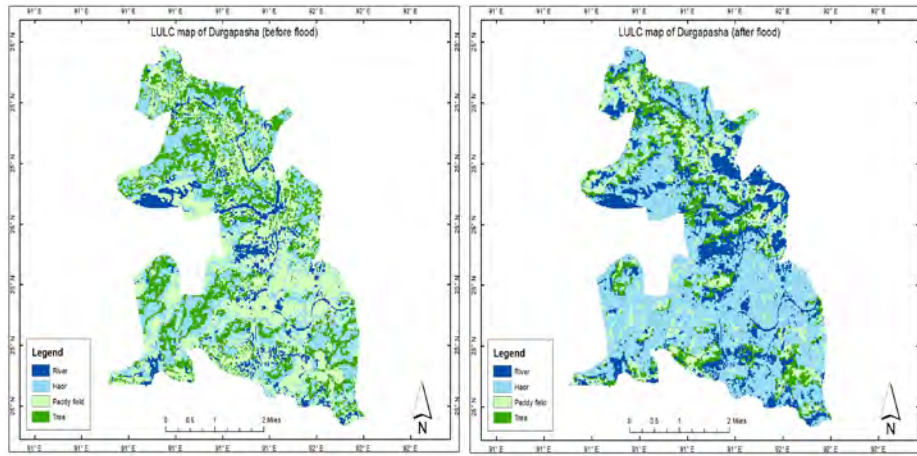


Figure 8. LULC map of Durgapasha before and after flood. Source: Authors (2023).

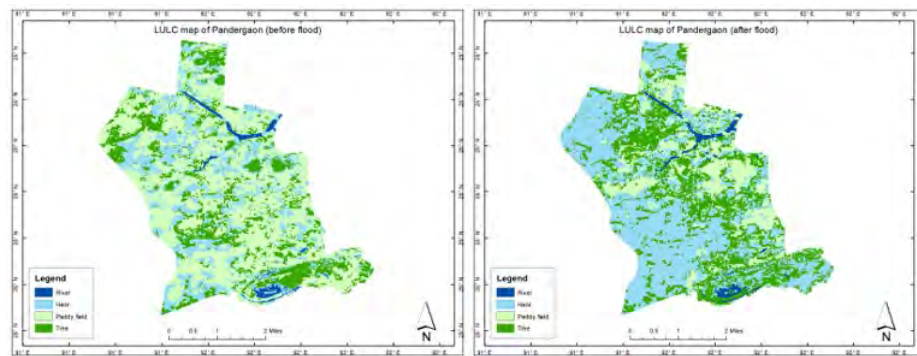


Figure 9. LULC map of Pandergaon before and after flood. Source: Authors (2023).

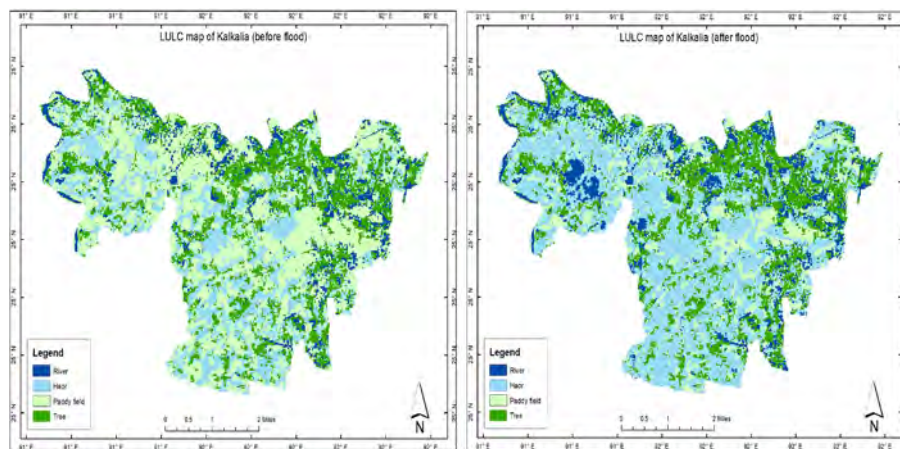
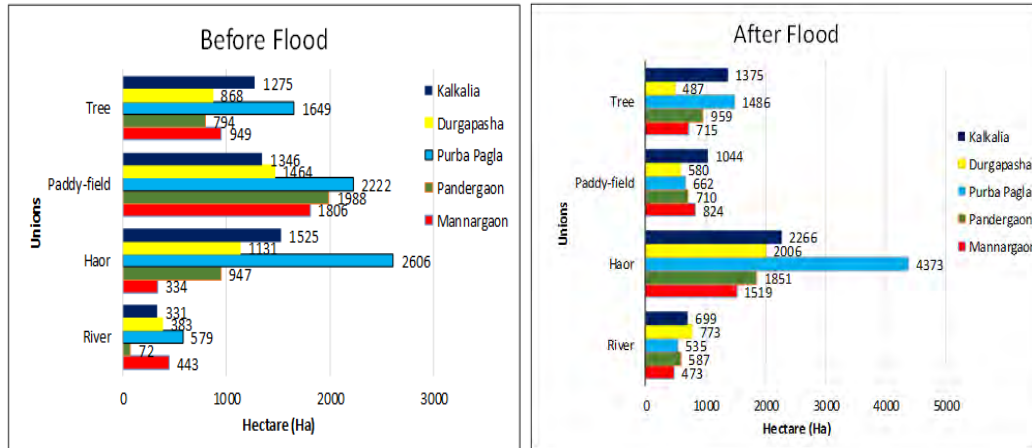


Figure 10. LULC map of Kalkalia before and after flood. Source: Authors (2023).

The bar chart in Figure 11 shows the area of land in hectares in the four land cover categories in the five unions before and after the flood.



**Figure 11.** Calculated areas of every union and their classes before and after flood.  
Source: Authors (2023).

### 3.1.4 Flooded paddy field area

The statistics of total agricultural areas which were flooded are given in Table 5 below. Purba Pagla, which had the largest area under paddy cultivation, also had the highest percentage of inundated crops at 52 percent. Least affected were Mannargaon and Kalkalia with around a third of the crops affected.

**Table 5.** Percentage of inundated paddy fields.

| Union       | Total paddy field (ha) | Flooded paddy field (ha) | Area (%) |
|-------------|------------------------|--------------------------|----------|
| Mannargaon  | 1,806                  | 539                      | 30       |
| Pandergaon  | 1,988                  | 930                      | 47       |
| Purba Pagla | 2,222                  | 1147                     | 52       |
| Durgapasha  | 1,464                  | 662                      | 45       |
| Kalkalia    | 1,346                  | 466                      | 35       |

### 3.1.5 Estimated agricultural economic loss calculation

According to World Data Atlas (Knoema, n.d.), the yield of rice per hectare was 48,667 kg in Bangladesh. This amounts to, on average, 4.87 tonnes of rice on an area of one ha. On average, a tonne of rice costs Tk. 47,500 (Ahmed, 2022). Therefore, it is estimated that 3,744 ha agricultural land being inundated resulted in damage of Tk. 864 million worth of crops during flood event across the study area.

**Table 6.** Calculated economic loss for crops.

| Union       | Total paddy field (ha) | Flooded paddy field (ha) | Estimated loss of yield (tonne) | Equivalent economic loss (millions of Tk.) |
|-------------|------------------------|--------------------------|---------------------------------|--|
| Mannargaon  | 1,806                  | 539                      | 2,625                           | 124  |
| Pandergaon  | 1,988                  | 930                      | 4,529                           | 215  |
| Purba Pagla | 2,222                  | 1,147                    | 5,586                           | 265  |
| Durgapasha  | 1,464                  | 662                      | 3,224                           | 153  |
| Kalkalia    | 1,346                  | 466                      | 2,269                           | 107  |

### 3.2. Discussion

The research aimed to establish a technique that utilizes optical and radar image analysis in GEE platform to reduce computation time and resource requirements, high dependency on field data collection, precise land use mapping and quantified flood damage assessment. The highest area covered by floods was 3,566 ha, according to the results shown in Table 3. Despite having this much land flooded, Purba Pagla stands in second place due to the comparison with respect to its total area. Kalkalia had the most inundated land in relation to its total area, with 53% of its land inundated. Purba Pagla, is the largest union, accounting for 50% of the total area. Though Mannargaon Union was the least flooded, it had 1,048 ha of land underwater. Figure 5 depicts an approximation in the flooded area for a comparative analysis between the simulated map created in the study and the secondary map provided by FFWC. It was calculated that 13% of the flood map results among the unions were dissimilar on average. This study demonstrates that it is possible to produce a quick and viable flood map utilizing freely available satellite images and open analysis platforms like earth engine. This allows for earlier detection of inundated areas, which aids in mitigation and preparedness. Long-term flood extent mapping can result in safe shelters and evacuation sites, as well as decision-making and flood management activities. Real-time inundation maps are critical for relief operations (Uddin et al., 2019).

The pre- and post-flood LULC classified map results in Figures 6 to 10 show that the paddy fields and tree-covered areas decreased among unions after the catastrophic flood. In contrast, river and haor areas increased.

According to KII, the three upazilas were stranded by flood for approximately fifteen days. Thousands of hectares of vegetation were lost during this time, and the affected population was evacuated to higher areas until the river level dropped and water began to drain out. According to the officers' estimates, Purba Pagla, Durgapasha, and Kalkalia had all lost a significant amount of vegetation, with Purba Pagla losing the most. Mannargaon and Pandergaon unions of Dowara bazaar upazila were the least affected, with Pandergaon losing the least amount of vegetation. It was stated that during the pre-monsoon season, due to early forecasting of flood events, farmers were able to quickly cultivate crops beforehand. Thorough union level LULC assessment, pre and post flood area calculation for paddy field impact utilizing combination of SAR data, optical data, and secondary data in GEE, ERDAS Imagine and ArcGIS platform have not yet been

done for Sunamganj, Bangladesh.

Challenges for flood extent mapping include data unavailability and incorrect data which causes difficulties in isolated or poorly supervised areas (Notti et al., 2018). When using Sentinel 2 data for LULC map, cloud coverage over the study area can hide multispectral data from the surface. As the signal cannot penetrate through clouds, it can lower the quality of acquired data for LULC analyses and will need additional cloud removal approaches to be implemented (Chormanski et al., 2011). Flood extent mapping using Sentinel 1 data failed to identify four of the 20 selected locations as flooded (according to the KII, all twenty landmarks were inundated). As shown in Table 6, Purba Pagla suffered the greatest economic loss from damage of standing rice crop, while Kalkalia experienced the least. In this study, threshold techniques were used to detect inundated areas, the results may vary from the actual estimation. The threshold values were chosen depending on physical observations and differences in pixel values, there is the possibility of some pixels being misclassified (Singha et al., 2020). The time series analysis of LULC damage pattern alteration in the study area with the variation of flooding intensity from past image analysis can help establish a trend of change in impact of the paddy field due to flooding.

#### 4. Conclusion

The division of Sylhet was severely flooded during the 2022 monsoon season. In this research, five unions of Sunamganj district with a history of flooding were chosen as the study area. The GEE platform has proven to be promising for quick analyses during flood events due to its automatic generation maps and instantaneous execution of analytical commands (Tiwari et al., 2020). With the aid of GEE and GIS, this study created a map that depicted the extent of flooding in the study area. Statistics of inundated areas were computed for both the secondary map provided by FFWC and the generated map using raster calculation and threshold techniques. The calculations for both maps were compared and found to have a good match.

This type of study can enable quick assessment of the degree of loss caused by unexpected flooding to various land use categories without the need for physical inspections or on-site assessments. This condensed strategy can be an effective tool for disaster management because it is cost and time efficient. By calculating the flooded area for each type of land cover, the extent of the damage can be immediately estimated. This information could be crucial for the emergency response team to enable effective resource allocation and prioritize relief activities because it provides a preliminary understanding of the impact on various land use types (Singha et al., 2020).

#### 5. References

- Ahmad, M. Y., & Munim, N. H. (2020). Approach of remote sensing and GIS techniques of land use and land cover mapping –Patna Municipal Corporation, (PMC) Patna, Bihar, India. *Current World Environment*, 15, 371–377. <https://doi.org/10.12944/cwe.15.2.25>
- Ahmed, T. (2022). *Grain and feed update: Bangladesh*. United States Department of Agriculture, Foreign Agricultural Service. [Report no. BG2023-0018]. [https://apps.fas.usda.gov/newgainapi/api/Report/DownloadReportByFileName?fileName=Grain%20and%20Feed%20Update\\_Dhaka\\_Bangladesh\\_BG2023-0018.pdf](https://apps.fas.usda.gov/newgainapi/api/Report/DownloadReportByFileName?fileName=Grain%20and%20Feed%20Update_Dhaka_Bangladesh_BG2023-0018.pdf)

- Aziz, M. A., Moniruzzaman, M., Tripathi, A., Hossain, M. I., Ahmed, S., Rahaman, K. R., Rahman, F., & Ahmed, R. (2022). Delineating Flood Zones upon Employing Synthetic Aperture Data for the 2020 Flood in Bangladesh. *Earth Systems and Environment*, 6(3), 733–743. <https://doi.org/10.1007/s41748-022-00295-0>
- Bangladesh Bureau of Statistics. (2022). *Population & housing census 2022: Preliminary report*. Bangladesh Bureau of Statistics.
- Bangladesh Red Crescent Society. (2022). Flash Flood 2022. *International Federation of Red Cross and Red Crescent Societies*.
- Bégué, A., Arvor, D., Bellon, B., Betbeder, J., de Aballeyra, D., Ferraz, R. P. D., Lebourgeois, V., Lelong, C., Simões, M., & Verón, S. R. (2018). Remote sensing and cropping practices: A review. *Remote Sensing*, 10(1), 1–32. <https://doi.org/10.3390/rs10010099>
- BSS. (2022, June 16). *Flood situation deteriorates in Sylhet, Sunamganj*. 1–2. <https://en.prothomalo.com/bangladesh/local-news/flood-situation-deteriorates-in-sylhet-sunamganj>
- Chormanski, J., Okruszko, T., Ignar, S., Batelaan, O., Rebel, K. T., & Wassen, M. J. (2011). Flood mapping with remote sensing and hydrochemistry: A new method to distinguish the origin of flood water during floods. *Ecological Engineering*, 37(9), 1334–1349.
- Cossu, R., Schoepfer, E., Bally, P., & Fusco, L. (2009). Near real-time SAR-based processing to support flood monitoring. *Journal of Real-Time Image Processing*, 4(3), 205–218. <https://doi.org/10.1007/s11554-009-0114-4>
- Dadhich, G., Miyazaki, H., & Babel, M. (2019). Applications of sentinel-1 synthetic aperture radar imagery for floods damage assessment: A case study of nakhon si thammarat, Thailand. *International Archives of the Photogrammetry, Remote Sensing and Spatial Information Sciences - ISPRS Archives*, 42(2/W13), 1927–1931. <https://doi.org/10.5194/isprs-archives-XLII-2-W13-1927-2019>
- Debu, D. (2023, July 2022). Water rising again in flood-hit Sunamganj. *The Business Standard*. <https://www.tbsnews.net/bangladesh/water-rising-again-flood-hit-sunamganj-451666>
- Dehni, A., & Lounis, M. (2012). Remote sensing techniques for salt affected soil mapping: Application to the Oran region of Algeria. *Procedia Engineering*, 33, 188–198. <https://doi.org/10.1016/j.proeng.2012.01.1193>
- Flood situation deteriorates in Sylhet, Sunamganj. (2022, June 17). *Prothom Alo*. <https://en.prothomalo.com/bangladesh/local-news/flood-situation-deteriorates-in-sylhet-sunamganj>
- Ge, G., Shi, Z., Zhu, Y., Yang, X., & Hao, Y. (2020). Land use/cover classification in an arid desert-oasis mosaic landscape of China using remote sensed imagery: Performance assessment of four machine learning algorithms. *Global Ecology and Conservation*, 22, e00971. <https://doi.org/10.1016/j.gecco.2020.e00971>
- GIS Cloud. (2020, July 2). *GIS mapping and benefits of online solutions*. <https://www.giscloud.com/blog/gis-mapping-and-benefits-of-online-solutions/>
- GIS Geography. (2023, October 23). *Google Earth Engine: A quick guide for beginners*. <https://gisgeography.com/google-earth-engine/>
- Gorsevski, P. V., Gessler, P. E., Foltz, R. B., & Elliot, W. J. (2006). Spatial prediction of landslide hazard using logistic regression and ROC analysis. *Transactions in GIS*, 10(3), 395–415.
- Hannan, K. A. (2021). Food Systems Summit 2021 Dialogues: Fifth Sub-national Dialogue in Sunamganj [official feedback form].



- <https://summitdialogues.org/dialogue/25580/official-feedback-25580-en.pdf?t=1626730030>
- Haque, M. I., & Basak, R. (2017). Land cover change detection using GIS and remote sensing techniques: A spatio-temporal study on Tanguar Haor, Sunamganj, Bangladesh. *Egyptian Journal of Remote Sensing and Space Science*, 20(2), 251–263. <https://doi.org/10.1016/j.ejrs.2016.12.003>
- Knoema (n.d.). Bangladesh – paddy rice yield. *World Data Atlas*. Retrieved 1 November, 2023, from <https://knoema.com/atlas/Bangladesh/topics/Agriculture/Crops-Production-Yield/Paddy-rice-yield>
- Mehmood, H., Conway, C., & Perera, D. (2021). Mapping of flood areas using Landsat with Google Earth Engine cloud platform. *Atmosphere*, 12(7), 866. <https://doi.org/10.3390/atmos12070866>
- Mishra, V. (2023, June 9). Weather alert: Heavy rain forecast for Assam in next 10 days. *Down To Earth*. <https://www.downtoearth.org.in/news/climate-change/weather-alert-heavy-rain-forecast-for-assam-in-next-10-days-89933>
- National River Conservation Commission. (2023). *Bangladesher nad-nadi sangya o sankhya* [Rivers of Bangladesh definition and number] National River Conservation Commission.
- Pandey, A. C., Kaushik, K., & Parida, B. R. (2022). Google Earth Engine for large-scale flood mapping using SAR data and impact assessment on agriculture and population of Ganga-Brahmaputra basin. *Sustainability*, 14(7), 4210. <https://doi.org/10.3390/su14074210>
- Rahman, M., Ningsheng, C., Mahmud, G. I., Islam, M. M., Pourghasemi, H. R., Ahmad, H., ... & Dewan, A. (2021). Flooding and its relationship with land cover change, population growth, and road density. *Geoscience Frontiers*, 12(6), 101224.
- Shermin, S. N. R. N. (2022). Identifying the effect of monsoon floods on vegetation and land surface temperature by using Google Earth Engine. *Urban Climate*, 43. <https://doi.org/10.1016/j.uclim.2022.101162>
- Singha, M., Dong, J., Sarmah, S., You, N., Zhou, Y., Zhang, G., Doughty, R., & Xiao, X. (2020). Identifying floods and flood-affected paddy rice fields in Bangladesh based on Sentinel-1 imagery and Google Earth Engine. *ISPRS Journal of Photogrammetry and Remote Sensing*, 166, 278–293. <https://doi.org/10.1016/j.isprsjprs.2020.06.011>
- Tanim, A. H., & Mullick, M. R. A. (2017). Application of synthetic aperture radar imagery for inundation mapping: A case of Sylhet flood event 2017. In *Proceedings of the International Conference on Risk Mitigation, 23–24 September, Dhaka*.
- Tassi, A., & Vizzari, M. (2020). Object-oriented LULC classification in Google Earth Engine combining SNIC, GLCM, and machine learning algorithms. *Remote Sensing*, 12(22), 3776. <https://doi.org/10.3390/rs12223776>
- Tiwari, V., Kumar, V., Matin, M. A., Thapa, A., Ellenburg, W. L., Gupta, N., & Thapa, S. (2020). Flood inundation mapping-Kerala 2018; Harnessing the power of SAR, automatic threshold detection method and Google Earth Engine. *PLoS One*, 15(8), e0237324. <https://doi.org/10.1371/journal.pone.0237324>
- Uddin, K., Matin, M. A., & Meyer, F. J. (2019). Operational flood mapping using multi-temporal Sentinel-1 SAR images: A case study from Bangladesh. *Remote Sensing*, 11(13). <https://doi.org/10.3390/rs11131581>
- United News of Bangladesh. (2022, June 10). Thousands in Sunamganj affected by second round of flooding. *New Age Bangladesh*. <https://www.newagebd.net/article/172893/thousands-in-sunamganj-affected-by-second-round-of-flooding>
- Zahid, O. (2022). *Living with floods and reducing vulnerability in Sylhet*. The Global Policy Institute.

<https://gpilondon.com/publications/living-with-floods-and-reducing-vulnerability-in-sylhet>

### **Appendix 1**

Link to javascript code for flood extent mapping on GEE platform:

<https://code.earthengine.google.com/aeaff25472d950b16f252c7fe5689d5a?noload=1>

### **Appendix 2**

Link to javascript code for land use land cover mapping on GEE platform:

<https://code.earthengine.google.com/c8aff2595f1fe16bcc33a4bbf4b7f86a>

### **Appendix 3**

Check list of information collected through the KIIs:

- Duration of flood event.
- Percentage of area inundated during peak flood days.
- Confirmation of whether the pinpointed landmarks of specific unions were under water as shown in the Upazila inundation map.
- Estimated number of cultivation land lost due to flood.